DOE/NASA/50112-75
NASA TM-100899

Testing of a Variable-Stroke Stirling Engine

Lanny G. Thieme
National Aeronautics and Space Administration
Lewis Research Center

and

David J. Allen
Sverdrup Technology, Inc.
NASA Lewis Research Center Group

Work performed for
U.S. DEPARTMENT OF ENERGY
Conservation and Renewable Energy
Office of Vehicle and Engine R&D

Prepared for the
21st Intersociety Energy Conversion Engineering Conference (IECEC)
cosponsored by the ACS, SAE, ANS, ASME, IEEE, AIAA, and AIChE
San Diego, California, August 25-29, 1986

DISCLAIMER

Printed in the United States of America

Available from
National Technical Information Service
U.S. Department of Commerce
5285 Port Royal Road
Springfield, VA 22161

NTIS price codes[1]
Printed copy: A02
Microfiche copy: A01

[1]Codes are used for pricing all publications. The code is determined by the number of pages in the publication. Information pertaining to the pricing codes can be found in the current issues of the following publications, which are generally available in most libraries: *Energy Research Abstracts (ERA); Government Reports Announcements* and Index (*GRA* and I); *Scientific and Technical Abstract Reports (STAR);* and publication, NTIS-PR-360 available from NTIS at the above address.

DOE/NASA/50112-75
NASA TM-100899

Testing of a Variable-Stroke Stirling Engine

Lanny G. Thieme
National Aeronautics and Space Administration
Lewis Research Center
Cleveland, Ohio 44135

and

David J. Allen
Sverdrup Technology, Inc.
NASA Lewis Research Center Group
Cleveland, Ohio 44135

Work performed for
U.S. DEPARTMENT OF ENERGY
Conservation and Renewable Energy
Office of Vehicle and Engine R&D
Washington, D.C. 20545
Under Interagency Agreement DE-AI01-85CE50112

Prepared for the
21st Intersociety Energy Conversion Engineering Conference (IECEC)
cosponsored by the ACS, SAE, ANS, ASME, IEEE, AIAA, and AIChE
San Diego, California, August 25-29, 1986

TESTING OF A VARIABLE-STROKE STIRLING ENGINE

Lanny G. Thieme
National Aeronautics and Space Administration
Lewis Research Center
Cleveland, Ohio 44135

and

David J. Allen
Sverdrup Technology, Inc.
NASA Lewis Research Center Group
Cleveland, Ohio 44135

E-3056

SUMMARY

In support of the U.S. Department of Energy's Stirling Engine Highway Vehicle Systems Program, NASA Lewis investigated the use of variable stroke as an alternative to the complex mean-pressure control system for controlling the power output of an automotive Stirling engine. The primary benefits offered by variable-stroke operation are a simpler control system, a possible part-load efficiency gain, and less static working-fluid leakage from the engine due to a lower number of connections to the working space. For this investigation, the Advenco Stirling engine was purchased from Philips Research Laboratories of the Netherlands. Testing of the Advenco at NASA Lewis has been completed.

The Advenco is a four-cylinder, double-acting engine designed for a maximum engine output of about 40 kW with hydrogen working fluid at a design mean compression-space pressure of 10 MPa. Variable-stroke operation is achieved with a variable-angle swash-plate drive system. The stroke can be varied from 10 mm at a 5° swash-plate angle to 48.5 mm at a 22° swash-plate angle.

The engine was tested for a total of about 70 hr with both helium and hydrogen working fluids and over a range of pressures, strokes, and engine speeds. The maximum brake power and brake gross thermal efficiency obtained were 10.0 kW and 22.1 percent, respectively. These values were recorded for a run at 5-MPa mean compression-space pressure with hydrogen working fluid and a 40-mm stroke.

Comparisons with computer simulation predictions indicated that the measured performance was lower than expected. It is felt that this was primarily due to excessive mechanical losses, as indicated by excessive heat rejected to the oil and by the occurrence of two drive-system failures.

Tests were performed to allow comparisons of part-load efficiencies obtained with variable-pressure and with variable-stroke operation. Both the test data and the computer simulation predictions showed a part-load efficiency gain with variable stroke that increased with increasing engine speed and was greater with helium working fluid than with hydrogen. This efficiency gain was primarily due to lower flow losses through the heat exchangers and to reduced heat losses that tended to decrease with reduced stroke and pressure ratio (such as shuttle losses). For automotive applications operating with

hydrogen working fluid and mainly at lower engine speeds, little or no gain in part-load efficiency would be expected.

Two failures with the variable-angle swash-plate drive system were encountered during the test program; these failures limited testing to the lower power levels. The failures are not thought to be caused by problems inherent in the variable-stroke concept but they do emphasize the need for careful design in the area of the crossheads where the failures occurred.

This paper summarizes the entire Advenco test program and presents detailed hydrogen test data and information on the second drive-system failure. The helium test results and a description of the first failure were presented in detail in an earlier test report (ref. 1).

INTRODUCTION

This testing at NASA Lewis was done in support of the U.S. Department of Energy (DOE) Stirling Engine Highway Vehicle Systems Program. The NASA Lewis Research Center, through interagency agreement DE-AI01-85CE50112 with DOE, is responsible for management of the project under the program direction of the DOE Office of Transportation Systems, Heat Engine Propulsion Division.

The power output of most kinematic Stirling engines is varied by changing the mean pressure level of the working fluid. To obtain the desired response for automotive applications, a relatively complex mean-pressure control system is required with attendant reliability and maintenance problems. Also, with this control system, the many connections to the working space add more potential leakage paths for the working fluid. While experience with the mean-pressure control system demonstrates very good performance, these possible problems have raised interest in investigating alternatives for controlling the power output of a Stirling engine.

This interest led to the purchase of the Advenco (Advanced Engine Concept) Stirling engine from Philips Research Laboratories of the Netherlands. This engine is a four-cylinder, double-acting engine designed for a maximum engine output of about 40 kW with hydrogen working fluid. The major difference between this and current kinematic Stirling engines is the use of variable stroke as a method of power control. The stroke is varied with a variable-angle swash-plate drive system.

The engine was installed in a test cell at NASA Lewis. The objectives of the Advenco testing were as follows:

(1) Evaluate the benefits of variable-stroke power control relative to mean-pressure control; compare the part-load efficiencies obtained with variable-stroke and variable-pressure operation

(2) Evaluate variable-angle swash-plate drive as a system for obtaining variable stroke

(3) Provide information to Stirling engine R & D companies for development of variable-angle swash-plate drive

(4) Obtain test data over a range of strokes to aid in the validation of Stirling engine computer simulations

The benefits of variable-stroke control with respect to mean-pressure control include reduced complexity of the power control system and a possible part-load efficiency gain. The use of the variable-stroke control system eliminates many potential working-fluid leakage paths associated with the mean-pressure control system. Also, if desired, it permits the use of a pressurized crankcase that may reduce the shaft-sealing problem.

This paper presents a summary of the Advenco test program at NASA Lewis. It briefly describes the Advenco engine and test setup, presents test results with helium and hydrogen working fluids, and discusses two engine failures that limited testing to low power levels. A detailed description of the engine and the test results obtained with helium working fluid were included in an earlier test report (ref. 1).

ENGINE DESCRIPTION

The Advenco engine is a four-cylinder, double-acting Stirling engine designed for a maximum output of about 40 kW with hydrogen working fluid. The Advenco was built by Philips Research Laboratories of the Netherlands. A variable-angle swash-plate drive system is used to vary piston stroke in order to control engine power output. The stroke can be varied from 10 mm at a 5° swash-plate angle to 48.5 mm at a 22° swash-plate angle. The design mean pressure level is 10 MPa. The efficiency was maximized at a part-power condition corresponding to a 14° swash-plate angle and a 4500-rpm engine speed.

Figure 1 is a photograph of the Advenco engine in its test facility at NASA Lewis. The engine is shown in cross section in figure 2. The Advenco engine has been described in detail in an earlier NASA test report (ref. 1) and also as originally manufactured by Philips Research Laboratories (ref. 2).

The variable-angle swash-plate assembly is shown in figure 3. The swash plate rotates with the main shaft. Its surface is made slightly convex to maintain line contact with the sliders. A balance ring is attached around the outside of the swash plate.

To change the angle of the swash plate, hydraulic fluid is ported through concentric channels in the main shaft to the vane-type rotary actuator mounted behind the swash plate. The hydraulic pressure forces the actuator to rotate relative to the main shaft. This rotation is transmitted by gears to the swash plate. The swash plate's rotation around a tilted section of the main shaft causes the swash-plate angle to change. Further explanation of the variable-angle swash-plate drive system can be found in reference 3.

Figure 4 shows a typical crosshead and sliders that serve as the attachment between the reciprocating rod and piston and the rotating swash plate. Oil lubrication is provided to both sides of the sliders. Figure 4 also shows the rollsock rod seal cartridge and rollsock rod seal used in the Advenco to seal off the high-pressure working fluid in the working space from the oil in the crankcase.

TEST FACILITY

The NASA Lewis test facility used in the initial Advenco testing with helium working fluid is described in detail in reference 1. These tests used natural gas as the fuel. The airflow was varied to control the heater temperature to the average of four thermocouples that measured heater-tube working fluid temperature. The natural gas fuel was controlled by a mechanical controller which varied the fuel flow to set the desired air-to-fuel ratio. The cooling-water inlet temperature was controlled to a constant value.

A direct-current dynamometer with a low-friction, oil-floated cradle-bearing system absorbed the engine power output; torque was measured with a load cell. Engine stroke was determined electronically from a linear variable differential transformer (LVDT) signal. The LVDT measured piston position and was attached to the rear of one of the crossheads.

The initial Advenco testing with helium working fluid ended with a major drive-system failure. Following the rebuilding of the engine, the test facility was modified prior to testing with hydrogen working fluid. These changes were made to ensure the desired air-to-fuel ratio and to increase the accuracy of the engine energy balance. Because the mechanical air-fuel controller was no longer providing a repeatable air-to-fuel ratio, it was replaced with an electronic control circuit. This circuit measured the airflow and then adjusted a gas-flow valve to give the correct fuel flow according to a programmed air-to-fuel ratio schedule, The fuel system was modified to use 98 percent pure methane instead of natural gas in order to give an improved knowledge of the heat input from the fuel. The yearly variation of the heating value with natural gas was about ± 5 percent.

TEST RESULTS

A static pressure decay test was made before each engine start to compare working fluid leakage with previous runs. After each engine start, standard warmup conditions were set and the engine was run for 30 min. Performance at these conditions was checked against results from previous runs to verify proper engine operation.

For all tests, the average heater-tube gas temperature was controlled to 625 °C and the cooling-water inlet temperature to 50 °C. To allow comparison of part-load efficiencies obtained with variable-stroke and variable-pressure operation, the Advenco was tested over a range of both pressures and strokes. For each mean pressure level, a series of runs was made at different engine strokes. For each engine stroke and pressure, the engine speed was varied over the range of 1500 to 3500 rpm in 500-rpm increments. The procedure that was followed was to start at the lower values of mean-compression space pressure and engine stroke and then progressively increase these parameters.

The results of the initial engine tests with helium working fluid are presented in reference 1. The maximum brake power and brake gross thermal efficiency curves obtained in these tests are shown in figure 5. Brake gross thermal efficiency was calculated by dividing the brake power by the heat input from the fuel (based on the lower heating value) times 100. This series of tests was ended by a major drive-system failure that occurred at 5-MPa mean

compression-space pressure, 40-mm stroke, and 3000-rpm engine speed. This failure and the subsequent engine repairs are described in the section "Drive-System Failures".

Following completion of the engine repairs, checkout runs were made with helium working fluid. Performance was very difficult to repeat during this testing; this led to modifications of the test facility that included the installation of a new air-to-fuel ratio control system and the changeover to methane fuel.

Performance testing was then started with hydrogen working fluid. The engine was tested over the range of engine strokes of 20 to 40 mm for mean compression-space pressures of 3 and 5 MPa and at strokes of 20 and 27 mm at 7 MPa pressure. Brake power and brake gross thermal efficiency for mean compression-space pressures of 3, 5, and 7 MPa are shown in figures 6, 7, and 8, respectively. The maximum brake power measured during these hydrogen tests was 10.0 kW for a 5-MPa mean compression-space pressure, a 40-mm engine stroke, and a 3500-rpm engine speed. The maximum brake gross thermal efficiency was 22.1 percent for the same pressure and stroke but for an engine speed of 2500 rpm. Error analyses for the measurements of brake power and brake gross thermal efficiency are included in the appendix.

Representative engine pressure ratios obtained with helium and hydrogen working fluids are shown in figure 9. The pressure ratio is the maximum compression-space pressure divided by the minimum compression-space pressure. The minimum and maximum pressures were measured in the pressurization and vent lines connecting the four cycles. These lines were isolated from the working-fluid cycles by check valves; the check-valve action causes the minimum and maximum cycle pressures to be stored in the pressurization and vent lines, respectively.

Comparisons of the test data with computer predictions indicate that the experimental values of power and efficiency are lower than was anticipated. This is shown in figure 10, which compares the predicted brake power with measured values for both hydrogen and helium working fluids. The predictions were generated with the NASA Lewis Stirling engine computer simulation described in reference 4. The differences between measured and predicted brake power could partly be due to higher-than-expected mechanical losses, as evidenced by the drive-system failures (see the section "Drive-System Failures") and by excessive amounts of heat rejected to the oil lubricant. A comparison of the predicted mechanical losses with the heat rejected to the oil is shown in figure 11 for operation at 5-MPa pressure and 34-mm engine stroke and with hydrogen working fluid. The heat rejected to the oil was greater than the total predicted mechanical losses; the predicted mechanical losses also include piston ring friction that represents heat that is not rejected to the oil lubricant. It appears, then, that the actual mechanical losses were much greater than those used to generate the predictions. These unknown mechanical losses make comparisons with computer simulation predictions difficult at best.

The data were used to evaluate possible part-load efficiency gains with variable stroke. Figures 12 and 13 compare brake gross thermal efficiencies at part loads obtained by varying the stroke at constant pressure and by varying the pressure at constant stroke for hydrogen and helium working fluids, respectively. In both figures, the varying stroke curves are plotted for a constant pressure of 5 MPa. In figure 12, the varying pressure curves

for hydrogen are for a constant stroke of 40 mm; for the helium curves of figure 13, the constant stroke was 34 mm. The helium data were taken prior to the first drive-system failure.

For the limited amount of test data available, the efficiencies obtained with hydrogen working fluid at the lower engine speeds are identical for both variable-stroke and variable-pressure operating modes. At the higher engine speeds, the variable-stroke mode shows some improvement in the part-load efficiency. However, for the automotive application, little efficiency gain would be realized because the majority of operation is at the lower engine speeds. In figure 13, the variable-stroke mode with helium working fluid compared with the variable-pressure mode shows a greater improvement than for the hydrogen curves.

The efficiency improvements for variable-stroke operation compared with the variable-pressure mode at the same power level are due in part to lower flow losses through the heat exchangers for a given part-load point. This was predicted by the NASA Lewis Stirling engine computer simulation. In addition, heat losses that tend to decrease with reduced stroke and pressure ratio (such as shuttle losses) contribute to this improvement in efficiency. The larger difference between the variable-stroke and variable-pressure modes for helium working fluid (compared with hydrogen) may be reduced in an engine that was designed for helium (for example, heat exchangers designed for lower flow losses).

The test data used in figures 12 and 13 were restricted to the lower power levels. The NASA Lewis Stirling engine computer simulation was used to generate similar comparisons at the maximum stroke of 48.5 mm and the maximum pressure of 10 MPa. These comparisons are shown in figure 14. For these curves, the maximum brake power (1.0 on x-axis) was 43.2 kW for hydrogen and 24.2 kW for helium. The maximum brake thermal efficiency (1.0 on y-axis) (does not include burner losses) was 45 percent for hydrogen and 40 percent for helium. The same types of variations seen with speed and between hydrogen and helium in figure 14 were obtained for the actual test data shown in figures 12 and 13.

A variable-stroke engine is intended to operate constantly at its maximum working-space pressure. Thus, for the same design life, its pressure vessel walls tend to be thicker than those for a mean-pressure control engine with the same maximum pressure. This should give somewhat lower conduction losses for the comparable mean-pressure control engine; figures 12 through 14 have not been adjusted for this. It is not anticipated that this correction would be significant or change the conclusions based on the results obtained.

The testing with hydrogen working fluid was ended by another drive-system failure, this one much less severe than the first failure. This second failure occurred while running at 7-MPa pressure and a 1500-rpm engine speed while increasing the stroke from 27 to 34 mm. Approximately 45 hr of engine testing were accomplished with the engine after the rebuilding following the first failure. Both engine failures are reviewed in the following section.

Drive-System Failures

To gain the benefits of variable-stroke control, a workable drive system must be achieved. The Advenco engine uses the variable-angle swash-plate drive system that was briefly discussed in the section "Engine Description". During the 70 hr of Advenco engine testing at NASA Lewis, two drive-system failures were encountered.

The first was a major failure that occurred after about 25 hr of engine testing. The engine test conditions at the time were 5-MPa mean compression-space pressure with helium, 40-mm engine stroke, and 3000-rpm engine speed. This failure is described in detail in reference 1.

This first failure began when one of the crossheads began binding in its bore. The crossheads were made of high-strength aluminum with, at that time, a steel sleeve shrink-fitted over the end pieces. As the friction increased, the steel sleeve seized in its bore and was pulled off the crosshead. The consequent deflection of the crosshead freed the sliders from their retainer cups (see fig. 4) and allowed the sliders to scratch and gouge various drive-system parts. The unbalanced load caused by the loss of one crosshead overloaded the thrust bearing. When the bearing support failed, the main shaft moved rearward and broke the rear crankcase at its connection to the front crankcase section. Figure 15 shows the damaged rear crankcase with the crosshead sleeve stuck in its bore. This was the initial event of the failure.

The primary cause of this failure was determined to be misalignment of the crosshead bores in the two crankcase sections. This misalignment would have greatly increased the loading on the crossheads. Inadequate oil lubrication in the crosshead bores was also suspected. The original design made no specific provision for bringing oil directly to the crosshead-bore interface but rather relied on splash lubrication of the crosshead when the crosshead was out of its bore.

The following repairs were made to the engine to correct these problems:

(1) Spare front and rear crankcase sections were used in the rebuild. After detailed inspection procedures were completed, the crosshead bores of the rear crankcase were increased by about 0.50 mm to give the best possible alignment between the bores of the two crankcase sections.

(2) Spare crossheads were modified to fit the new crosshead dimensions. Rather than being sleeved, the crossheads were plated with silver with a flashing of tin for friction and wear characteristics. Their edges were rounded to minimize oil removal as the crosshead enters the bore.

(3) Pressurized lubrication was provided to the crosshead bores of the rear crankcase by installing direct feeds to the rear of these bores.

(4) As a possible aid in detecting problems before catastrophic failure, thermocouples were added in the walls of the crosshead bores of the rear crankcase.

The second drive-system failure occurred after about 45 hr of testing following the completion of the above repairs. This happened while running at 7-MPa pressure with hydrogen and a 1500-rpm engine speed upon increasing the

stroke to 34 mm. One of the crossheads momentarily seized in its bore and then freed itself, allowing the engine to be safely motored to a stop. The damage to the engine was primarily limited to this one crosshead and its two bores.

Two views of the failed crosshead are shown in figure 16. Removal of the silver plating can clearly be seen on the right end of the crosshead; this end rides in the bore of the rear crankcase. Analysis of the failure indicated the cause to be wear in the silver plating and/or a bonding failure of a plasma-sprayed aluminum coating used to build up the outer diameter of the rear end of the crosshead (before the silver was applied). The diameter of the crosshead had to be increased because of the need for enlarging the rear crankcase bores to provide the best possible alignment. The large chip off the extreme right end of the crosshead in the upper photo shows removal of the aluminum coating and the silver plating. Wear patterns in the silver were also evident on the other three crossheads; these could have resulted from the failure or from the wear during the 45 hr of testing. These three crossheads are shown in figure 17.

The only other damage found was a rotation, with respect to the main shaft, of the tilted hub around which the swash plate rotates to change its angle. This rotation caused a decrease in the minimum stroke of the engine.

Because of the nature of the crosshead plating and possibly because of the relieving action of the tilted hub's rotation, this failure was not as sudden as the first failure and caused much less damage. Also of interest was the response of the thermocouples in the walls of the crosshead bores. The wall temperature of the failed bore rose about 120 °C during the failure; this should be sufficient to allow these thermocouples to be used for automatic shutdowns.

CONCLUDING REMARKS

For automotive applications, variable-stroke power control offers reduced control system complexity. However, to achieve this benefit, a workable drive system must be obtained. It is not thought that the failures at NASA Lewis with the Advenco engine indicate any inherent problems with the variable-stroke concept but rather that these failures were related to restrictions of a hardware- and dollar-limited program. However, the failures do emphasize the need for careful design in the area of the crossheads. The crossheads require properly aligned bores and the careful selection of compatible materials for the crosshead and bore that can meet the requirements of life and engine balance.

From the limited test data that were obtained, only a small benefit, if any, could be expected in part-power efficiency for automotive applications that require operation primarily at low engine speeds. An application that requires substantial high-speed operation as well as operation over a range of loads may benefit to a greater extent.

After a review of the last failure, Advenco testing at NASA Lewis was stopped. Budget and manpower limitations were traded off with the probability of achieving enhanced performance in a limited time with the available hardware. Also, satisfactory progress was being made with the mean-pressure control system. Though no further work is planned, NASA Lewis does continue

to have an interest in the variable-stroke concept. Development by a private manufacturer of a more advanced version of a variable-stroke engine using a variable-angle swash-plate drive will be followed with interest. Also, the reliability of the mean-pressure control system will continue to be monitored.

APPENDIX - ERROR ANALYSIS FOR HEAT INPUT, BRAKE POWER, AND BRAKE GROSS THERMAL EFFICIENCY

An error analysis was done to determine the accuracy of the measured heat input, brake power, and brake gross thermal efficiency. Included in this appendix are a listing of the measurement accuracies, sample calculations of the uncertainties, and the results for representative high-power and low-power data points. An error analysis for the Advenco Stirling engine was done originally to see which measurements could be improved to decrease calculation uncertainties and also to understand these effects on the repeatability of the data. The error analysis led to some of the facility modifications mentioned in this report. The methane fuel system was installed and a lower range flowmeter for the fuel was purchased. The calculations shown in this appendix indicate the final results after the facility modifications.

For each measurement, the root-mean-square (rms) method was chosen to sum the individual errors in series from the instrument itself to the recording system. The measurement accuracies are listed in table I. Sample calculations of the uncertainties in the heat input, brake power, and brake gross thermal efficiency are shown for a high-power data point. The engine operating conditions for this data point are listed in table II.

The results of the error analysis are given in table III for two representative data points - the high-power point (10 kW) used in the sample calculations, and a low-power point (2 kW). The engine operating conditions for both points are listed in table II. These results indicate that the uncertainties for the higher power data are reasonable, with larger uncertainties associated with the low-power points. It should be noted that the maximum power obtained during the Advenco testing was only about 25 percent of the design output.

The standard calculation that was used for finding the uncertainty is given by the following equation (ref. 5):

$$w_R = \left[\left(\frac{\partial R}{\partial x_1} w_1\right)^2 + \left(\frac{\partial R}{\partial x_2} w_2\right)^2 + \ldots + \left(\frac{\partial R}{\partial x_n} w_n\right)^2\right]^{1/2} \qquad (1)$$

where

w_R uncertainty in the result R

$x_1, x_2, \ldots x_n$ independent variables

$w_1, w_2, \ldots w_n$ uncertainties in the independent variables

Sample calculations (for the high-power point listed in table II) are as follows:

Heat Input

$$Pwrin = Fflom \cdot LHV \cdot 4.184 \qquad (2)$$

where

Pwrin power into the engine, kW

Fflom fuel flow, g/sec

LHV lower heating value of the fuel, kcal/g
For methane, LHV = 11.955

$$w_{Pwrin} = \left[\left(\frac{\partial Pwrin}{\partial Fflom} \cdot w_{Fflom}\right)^2 + \left(\frac{\partial Pwrin}{\partial LHV} \cdot w_{LHV}\right)^2\right]^{1/2} \quad (3)$$

$$\frac{\partial Pwrin}{\partial Fflom} = LHV \cdot 4.184 \quad (4)$$

$$\frac{\partial Pwrin}{\partial LHV} = Fflom \cdot 4.184 \quad (5)$$

w_{Fflom} = (full-scale fuel-flow measurement) (measurement accuracy)

= 2.16 g/sec (0.010)

= 0.0216 g/sec (6)

w_{LHV} = 11.955 kcal/g (0.010)

= 0.11955 kcal/g (7)

$$w_{Pwrin} = \left[\left(LHV \cdot 4.184 \cdot w_{Fflom}\right)^2 + \left(Fflom \cdot 4.184 \cdot w_{LHV}\right)^2\right]^{1/2}$$

$$= \left[\left(11.955 \cdot 4.184 \cdot 0.0216\right)^2 + \left(1.05 \cdot 4.184 \cdot 0.11955\right)^2\right]^{1/2} \quad (8)$$

w_{Pwrin} = ±1.2 kW Measured power into the engine = 52.3 kW (9)

Percent error = ±2.3

Brake Power

Pwrout = Torq2 • RPM/9459.3 (10)

where

Pwrout brake power, kW

Torq2 engine torque, N-m

RPM engine speed, rpm

$$w_{Pwrout} = \left[\left(\frac{\partial Pwrout}{\partial Torq2} \cdot w_{Torq2}\right)^2 + \left(\frac{\partial Pwrout}{\partial RPM} \cdot w_{RPM}\right)^2\right]^{1/2} \quad (11)$$

$$\frac{\partial Pwrout}{\partial Torq2} = \frac{RPM}{9549.3} \quad (12)$$

$$\frac{\partial Pwrout}{\partial RPM} = \frac{Torq2}{9549.3} \quad (13)$$

w_{Torq2} = (full-scale torque measurement) (measurement accuracy)

= 101.7 N-m (0.0061)

= 0.6 N-m (14)

w_{RPM} = (full-scale engine speed measurement) (measurement accuracy)

= 6000 rpm (0.0014)

= 8.5 rpm (15)

$$w_{Pwrout} = \left[\left(\frac{RPM}{9549.3} \cdot w_{Torq2}\right)^2 + \left(\frac{Torq2}{9549.3} \cdot w_{RPM}\right)^2\right]^{1/2}$$

$$= \left[\left(\frac{3507}{9549.3} \cdot 0.6\right)^2 + \left(\frac{27.3}{9549.3} \cdot 8.5\right)^2\right]^{1/2} \quad (16)$$

w_{Pwrout} = ±0.2 kW Measured brake power = 10.0 kW (17)

Percent error = ±2.0

Brake Gross Thermal Efficiency

Brkeff = Pwrout • 100/Pwrin

(18)

where

Brkeff brake gross thermal efficiency, percent

Pwrout brake power, kW

Pwrin power into the engine, kW

$$w_{Brkeff} = \left[\left(\frac{\partial Brkeff}{\partial Pwrin} \cdot w_{Pwrin}\right)^2 + \left(\frac{\partial Brkeff}{\partial Pwrout} \cdot w_{Pwrout}\right)^2\right]^{1/2} \quad (19)$$

$$\frac{\partial Brkeff}{\partial Pwrin} = \frac{-100 \cdot Pwrout}{Pwrin^2} \quad (20)$$

$$\frac{\partial Brkeff}{\partial Pwrout} = \frac{100}{Pwrin} \quad (21)$$

$$w_{Pwrout} = 0.2 \text{ kW (from above)} \quad (22)$$

$$w_{Pwrin} = 1.2 \text{ kW (from above)} \quad (23)$$

$$w_{Brkeff} = \left[\left(\frac{-100 \cdot Pwrout}{Pwrin^2} \cdot w_{Pwrin}\right)^2 + \left(\frac{100}{Pwrin} \cdot w_{Pwrout}\right)^2\right]^{1/2}$$

$$= \left[\left(\frac{-100 \cdot 10.0}{52.3^2} \cdot 1.2\right)^2 + \left(\frac{100}{52.3} \cdot 0.2\right)^2\right]^{1/2} \quad (24)$$

$w_{Brkeff} = \pm 0.6$ percentage points

Measured brake gross thermal efficiency = 19.1 percent (25)

Percent error = ±3.1

REFERENCES

1. Thieme, L.G.: Initial Testing of a Variable-Stroke Stirling Engine. DOE/NASA/51040-58, NASA TM-86875, 1985.

2. Vos, J.: Design Characteristics of an Advanced Stirling Engine Concept. In Proceedings of the 14th Intersociety Energy Conversion Engineering Conference, Vol. 1, American Chemical Society, Washington, D.C., 1979, pp. 1191-1196.

3. Meijer, R.J.; and Ziph, B.: Variable Stroke Power Control for Stirling Engines. SAE Paper 810088, 1981.

4. Tew, Roy C., Jr.: Computer Program for Stirling Engine Performance Calculations. DOE/NASA/51040-42, NASA TM-82960, 1983.

5. Holman, J.P: Experimental Methods for Engineers, 2nd edition, McGraw-Hill, New York, 1971, p. 38.

TABLE I. - MEASUREMENT ACCURACIES IN PERCENT

Torque (load cell)	
Load cell system	0.6
Escort recording system	0.1
RMS value	0.61
Fuel flow (mass flowmeter)	
Flowmeter	1.0
Escort recording system	0.1
RMS value	1.0
Engine speed (magnetic pickup)	
Frequency-to-dc converter	0.1
Escort recording system	0.1
RMS value	0.14
Lower heating value (fuel)	
Methane	1.0

TABLE II. - ENGINE OPERATING CONDITIONS

[Fuel, methane; working fluid, hydrogen.]

Operating conditions	High-power point	Low-power point
Engine speed, rpm	3507	3006
Average heater gas temperature, °C	623	623
Cooling water inlet temperature, °C	49	49
Engine torque, N-m	27.3	6.4
Mean pressure, MPa	5.05	5.03
Engine stroke, mm	40.0	20.2
Fuel flow, g/sec	1.05	0.35
Power into the engine, kW	52.3	17.5
Brake power, kW	10.0	2.0
Brake gross thermal efficiency, percent	19.1	11.5

TABLE III. - UNCERTAINTY RESULTS FOR REPRESENTATIVE HIGH-POWER AND LOW-POWER DATA POINTS

(a) Power into the engine

	Power into the engine, kW	Uncertainty in the measurement, kW	Error, percent
High-power data point	52.3	1.2	2.3
Low-power data point	17.5	1.1	6.3

(b) Brake power

	Brake power, kW	Uncertainty in the measurement, kW	Error, percent
High-power data point	10.0	0.2	2.0
Low-power data point	2.0	0.2	10.0

(c) Brake gross thermal efficiency

	Brake gross thermal efficiency, percent	Uncertainty in the measurement, percentage points	Error, percent
High-power data point	19.1	0.6	3.1
Low-power data point	11.5	1.3	11.3

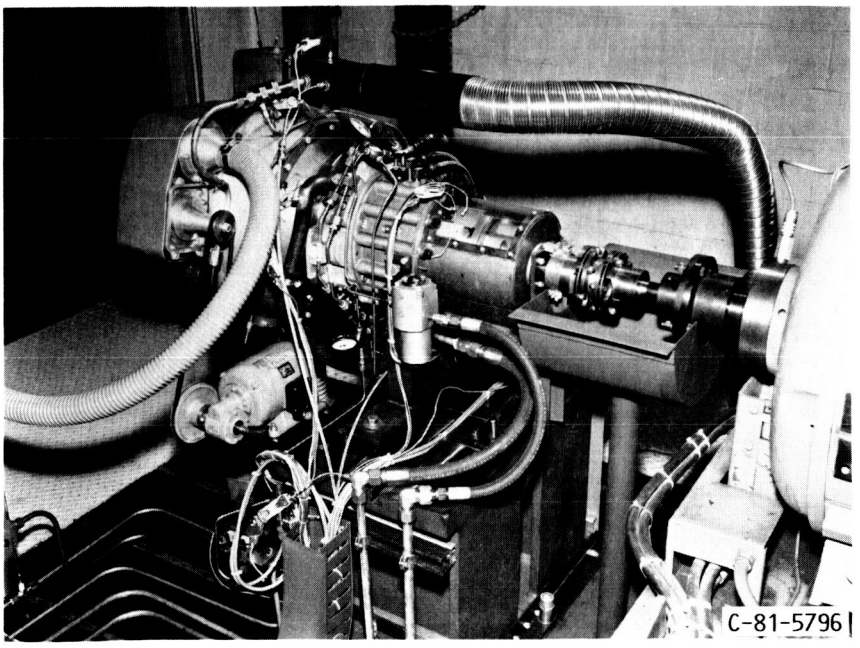

FIGURE 1. - ADVENCO STIRLING ENGINE.

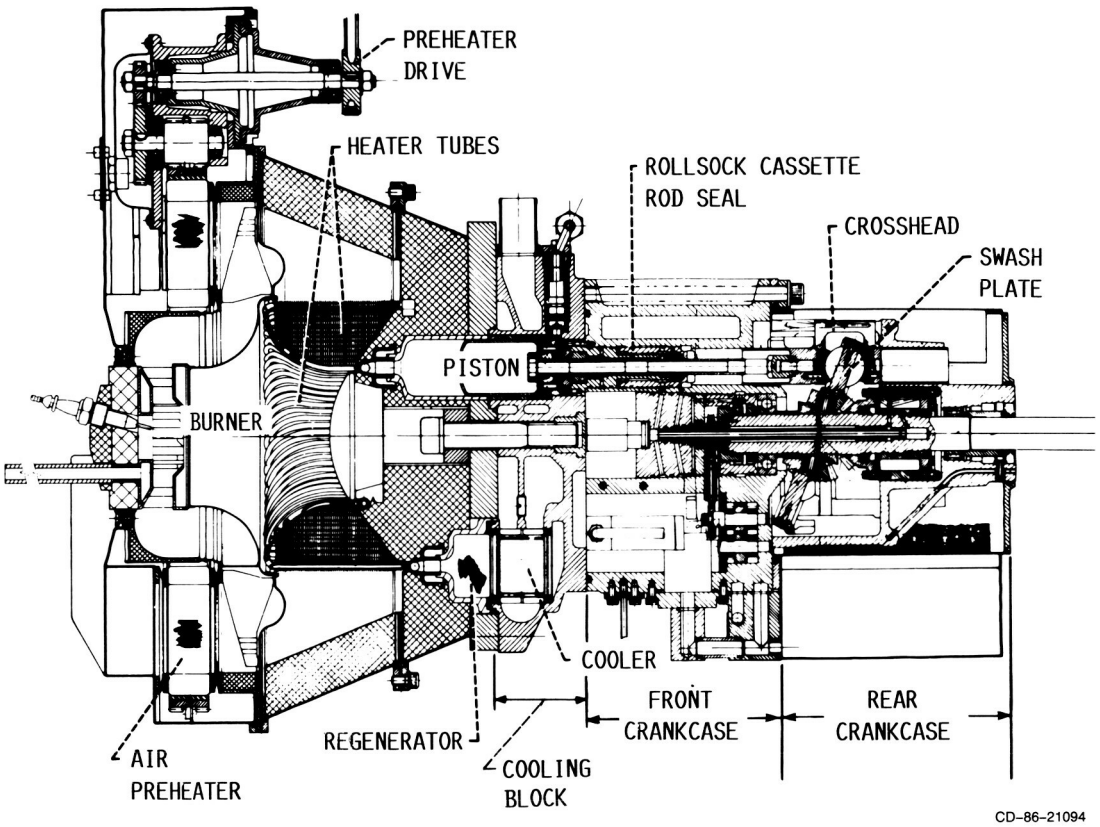

FIGURE 2. - ADVENCO STIRLING ENGINE CROSS SECTION.

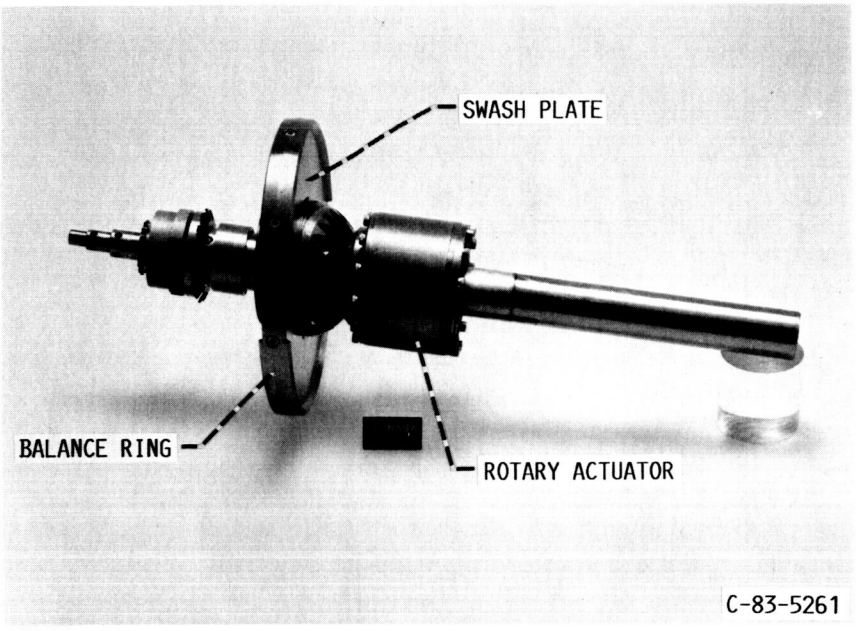

FIGURE 3. - VARIABLE-ANGLE SWASH-PLATE ASSEMBLY.

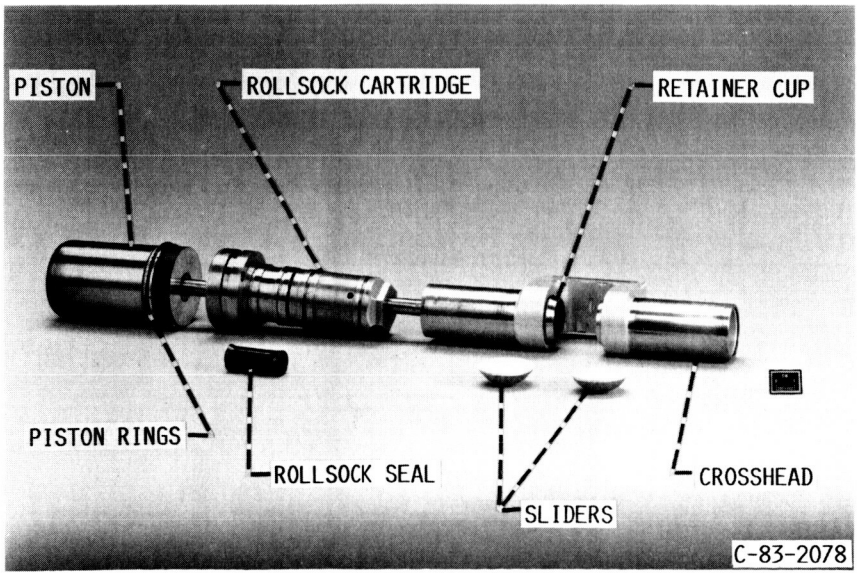

FIGURE 4. - PISTON, ROLLSOCK CARTRIDGE AND SEAL, AND CROSSHEAD WITH SLIDERS.

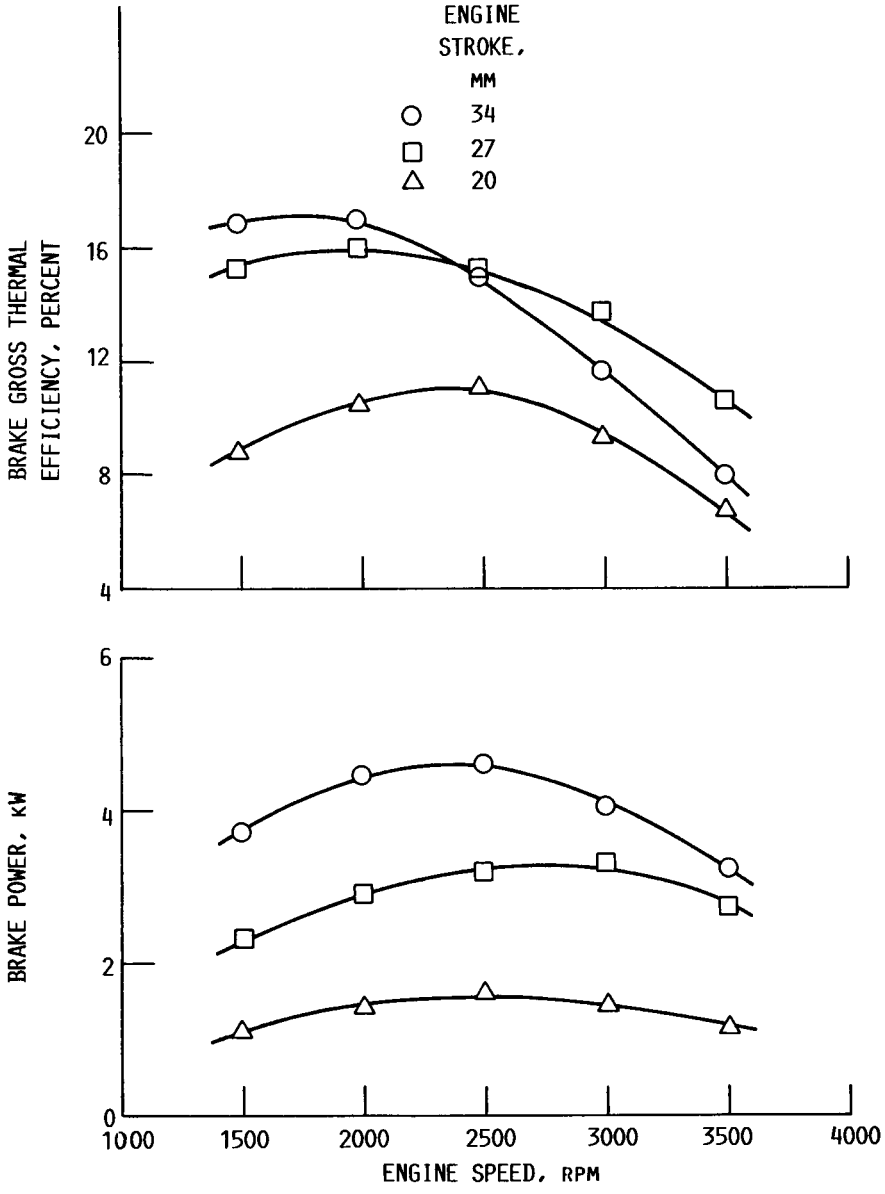

FIGURE 5. - ENGINE PERFORMANCE AS FUNCTION OF ENGINE SPEED AND ENGINE STROKE FOR MEAN COMPRESSION-SPACE PRESSURE OF 5 MPA. AVERAGE HEATER-TUBE GAS TEMPERATURE, 625 ^{O}C; COOLING-WATER INLET TEMPERATURE, 50 ^{O}C; HELIUM WORKING FLUID.

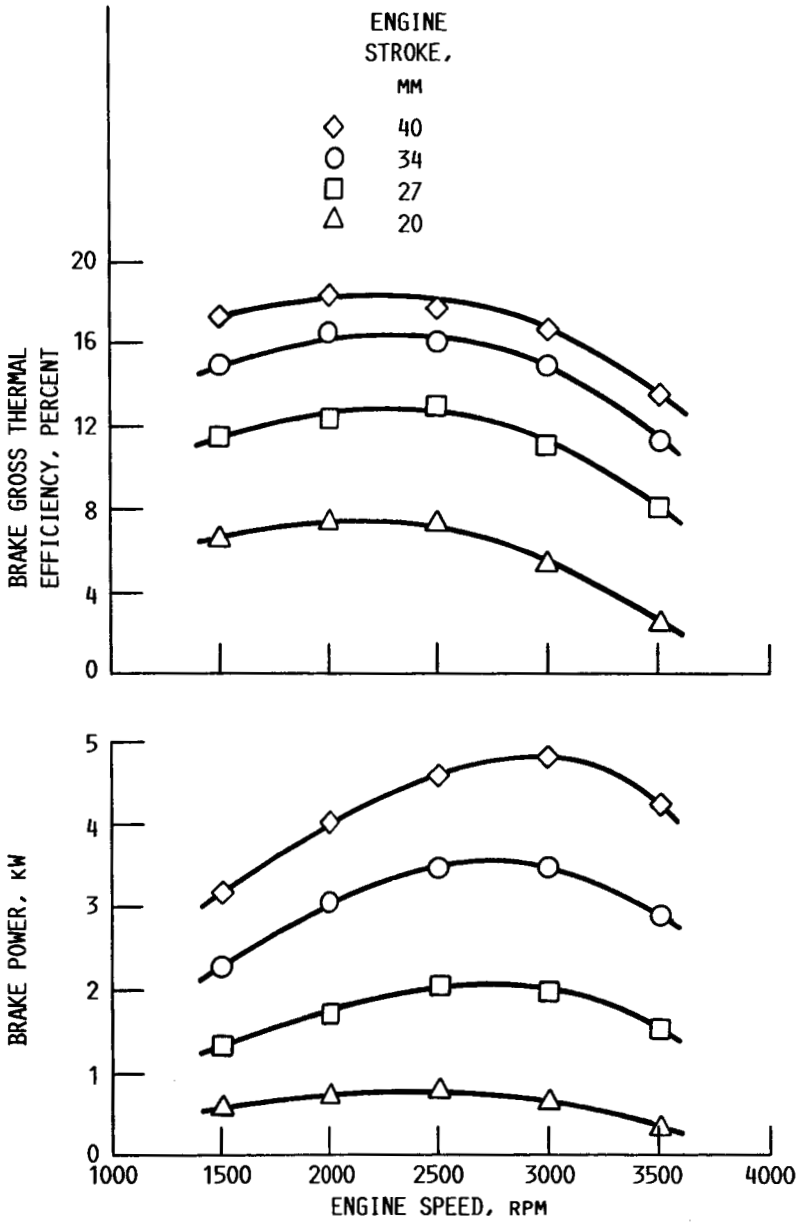

FIGURE 6. - ENGINE PERFORMANCE AS FUNCTION OF ENGINE SPEED AND ENGINE STROKE FOR MEAN COMPRESSION-SPACE PRESSURE OF 3 MPA. AVERAGE HEATER-TUBE GAS TEMPERATURE, 625 ^{o}C; COOLING-WATER INLET TEMPERATURE, 50 ^{o}C; HYDROGEN WORKING FLUID.

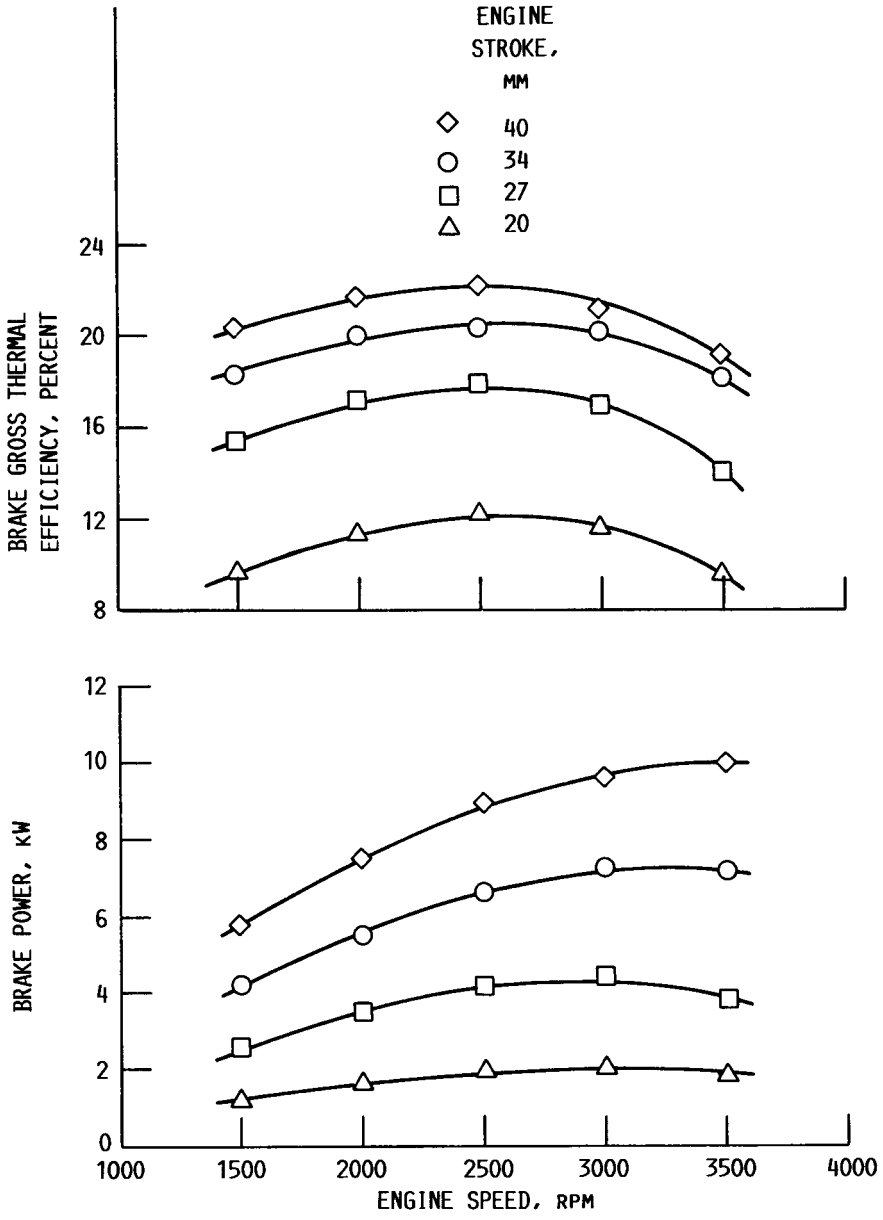

FIGURE 7. - ENGINE PERFORMANCE AS FUNCTION OF ENGINE SPEED AND ENGINE STROKE FOR MEAN COMPRESSION-SPACE PRESSURE OF 5 MPA. AVERAGE HEATER-TUBE GAS TEMPERATURE, 625 ^{o}C; COOLING-WATER INLET TEMPERATURE, 50 ^{o}C; HYDROGEN WORKING FLUID.

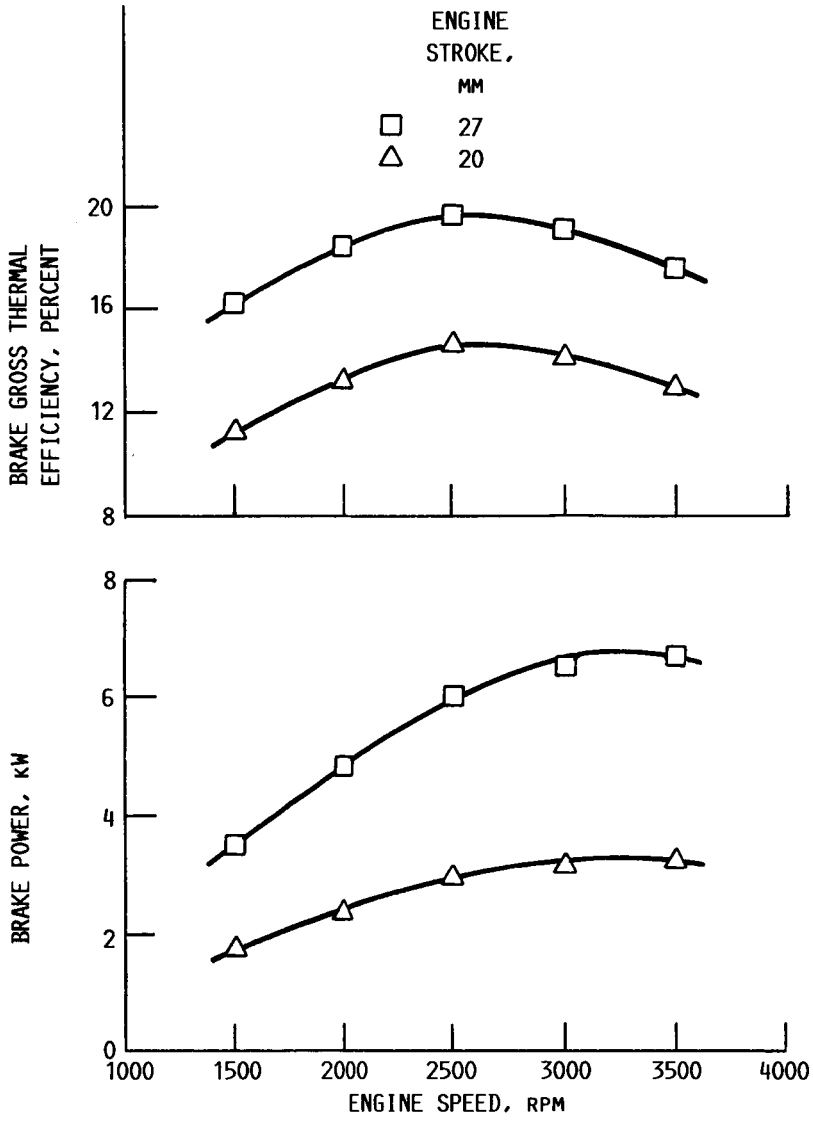

FIGURE 8. - ENGINE PERFORMANCE AS FUNCTION OF ENGINE SPEED AND ENGINE STROKE FOR MEAN COMPRESSION-SPACE PRESSURE OF 7 MPa. AVERAGE HEATER-TUBE GAS TEMPERATURE, 625 ^{o}C; COOLING-WATER INLET TEMPERATURE, 50 ^{o}C; HYDROGEN WORKING FLUID.

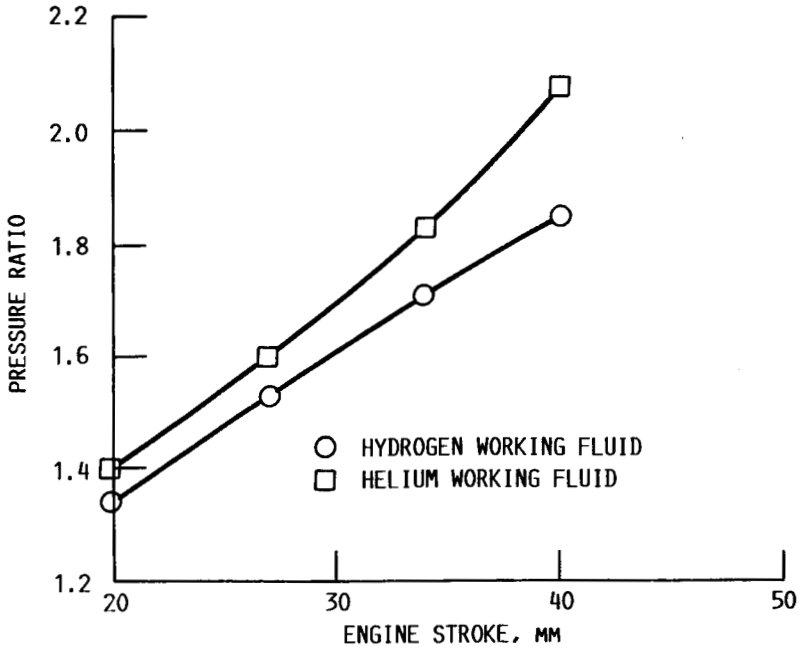

FIGURE 9. - RATIO OF MAXIMUM COMPRESSION-SPACE PRESSURE TO MINIMUM COMPRESSION-SPACE PRESSURE FOR HYDROGEN AND HELIUM WORKING FLUIDS AT VARIOUS ENGINE STROKES. MEAN COMPRESSION-SPACE PRESSURE, 3 MPA; ENGINE SPEED, 2500 RPM; AVERAGE HEATER-TUBE GAS TEMPERATURE, 625 ^{o}C; COOLING-WATER INLET TEMPERATURE, 50 ^{o}C.

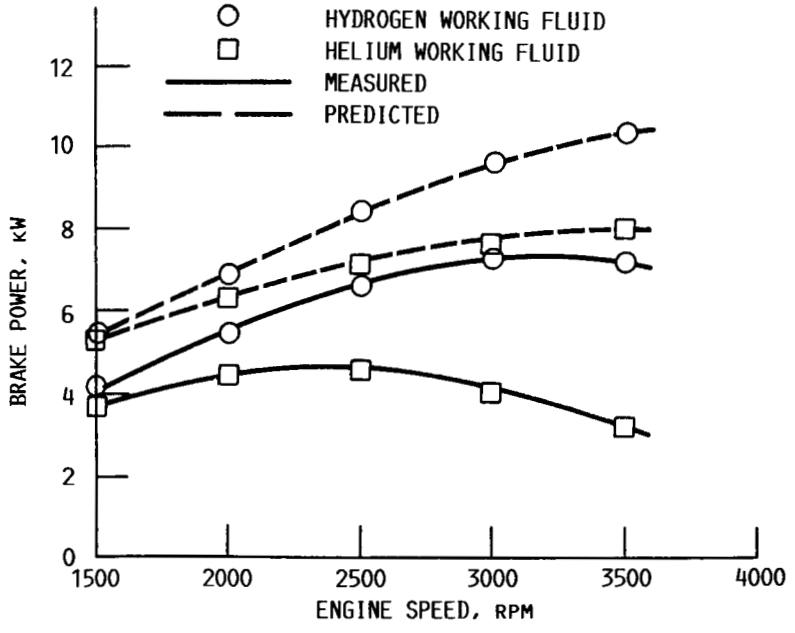

FIGURE 10. - COMPARISON OF MEASURED AND PREDICTED BRAKE POWER AT VARIOUS ENGINE SPEEDS FOR HELIUM AND HYDROGEN WORKING FLUIDS. MEAN COMPRESSION-SPACE PRESSURE, 5 MPA; ENGINE STROKE, 34 MM; AVERAGE HEATER-TUBE GAS TEMPERATURE, 625 ^{o}C; COOLING-WATER INLET TEMPERATURE, 50 ^{o}C.

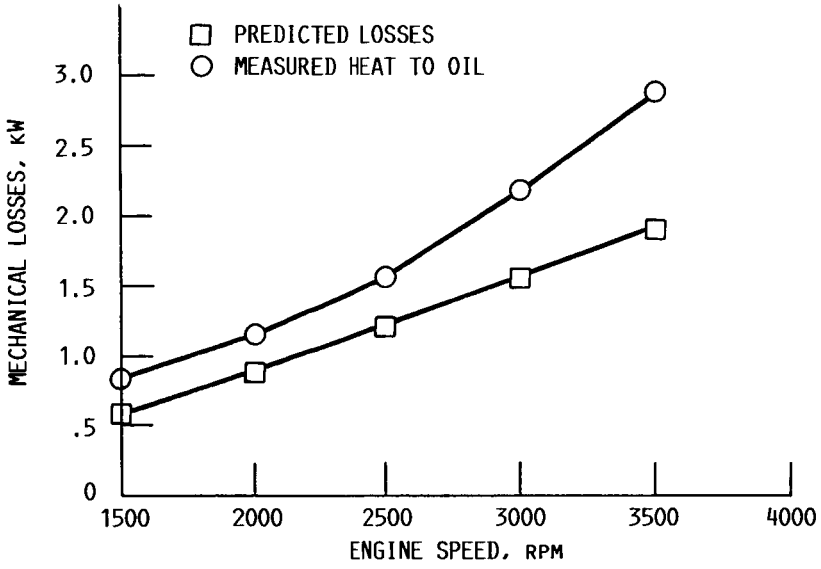

FIGURE 11.- COMPARISON OF MEASURED HEAT REJECTION TO OIL LUBRICANT WITH PREDICTED MECHANICAL LOSSES FOR VARIOUS ENGINE SPEEDS. MEAN COMPRESSION-SPACE PRESSURE, 5 MPa; ENGINE STROKE, 34 mm; AVERAGE HEATER-TUBE GAS TEMPERATURE, 625 ^{o}C; COOLING-WATER INLET TEMPERATURE, 50 ^{o}C; HYDROGEN WORKING FLUID.

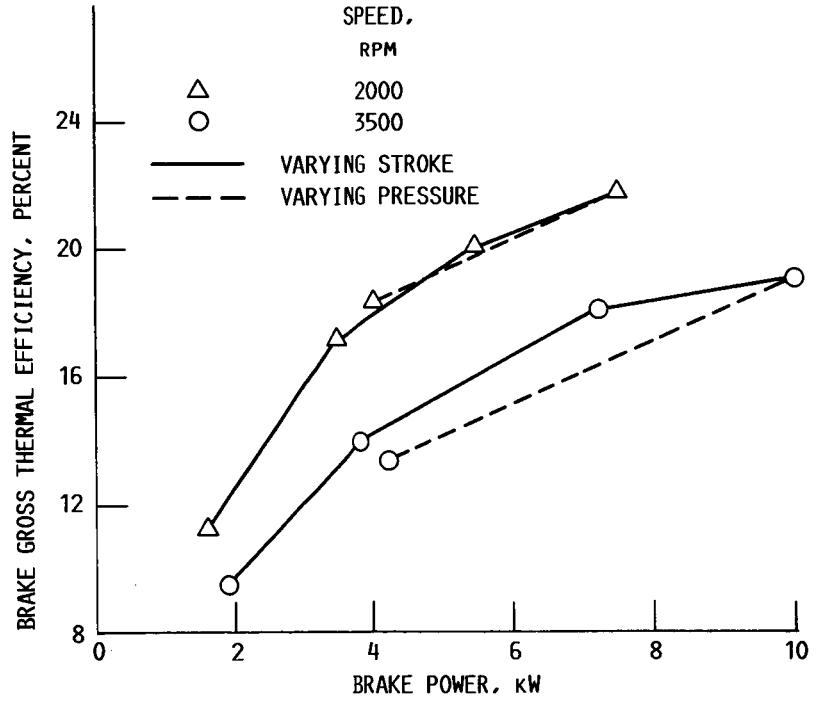

FIGURE 12. - COMPARISON OF EFFICIENCIES AT PART LOAD OBTAINED BY VARYING STROKE AT 5 MPa PRESSURE AND BY VARYING PRESSURE AT 40 mm STROKE; HYDROGEN WORKING FLUID.

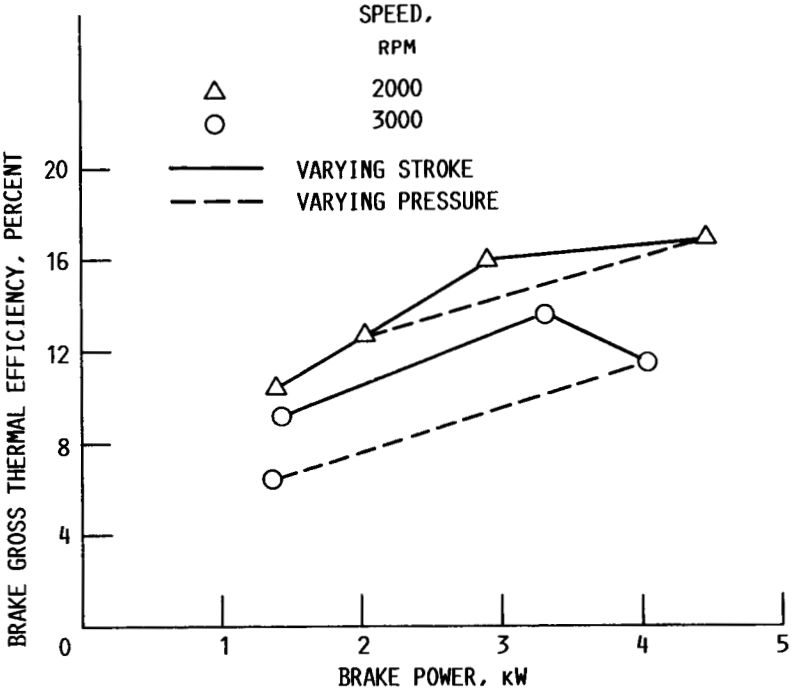

FIGURE 13. - COMPARISON OF EFFICIENCIES AT PART LOAD OBTAINED BY VARYING STROKE AT 5 MPa PRESSURE AND BY VARYING PRESSURE AT 34 mm STROKE; HELIUM WORKING FLUID.

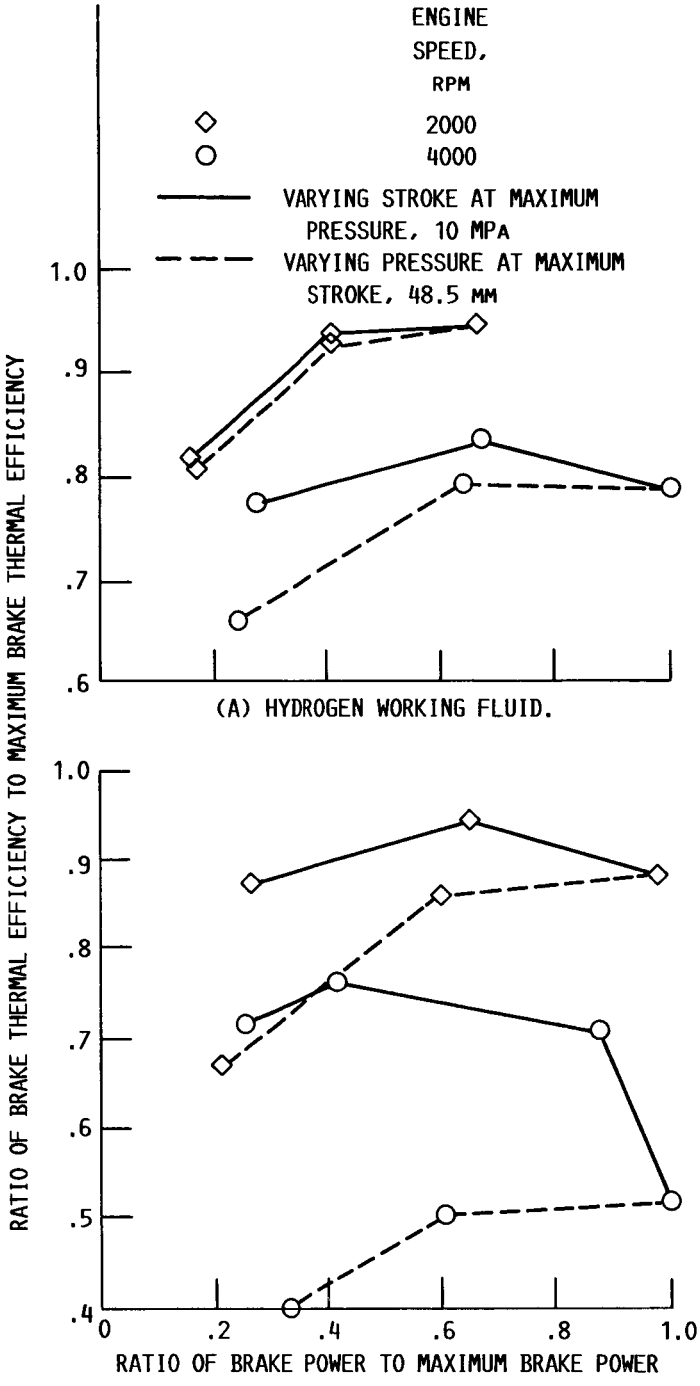

FIGURE 14. - COMPARISON OF COMPUTER SIMULATION PREDICTIONS OF PART-LOAD EFFICIENCIES.

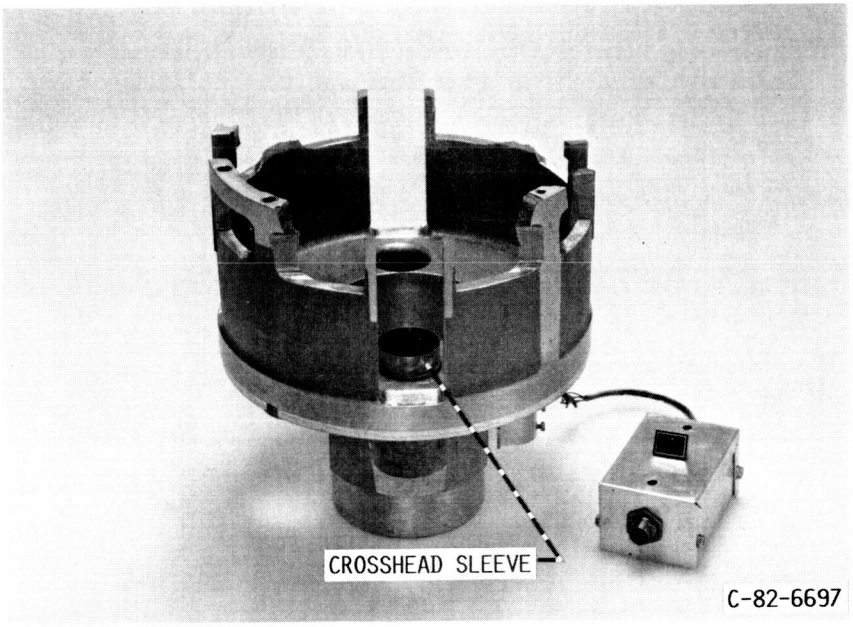

FIGURE 15. - DAMAGED REAR CRANKCASE FROM FIRST DRIVE-SYSTEM FAILURE; NOTE CROSSHEAD SLEEVE STUCK IN BORE.

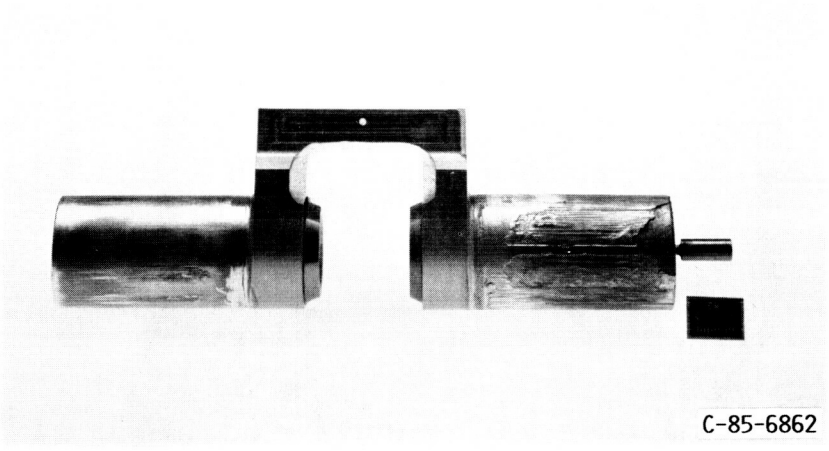

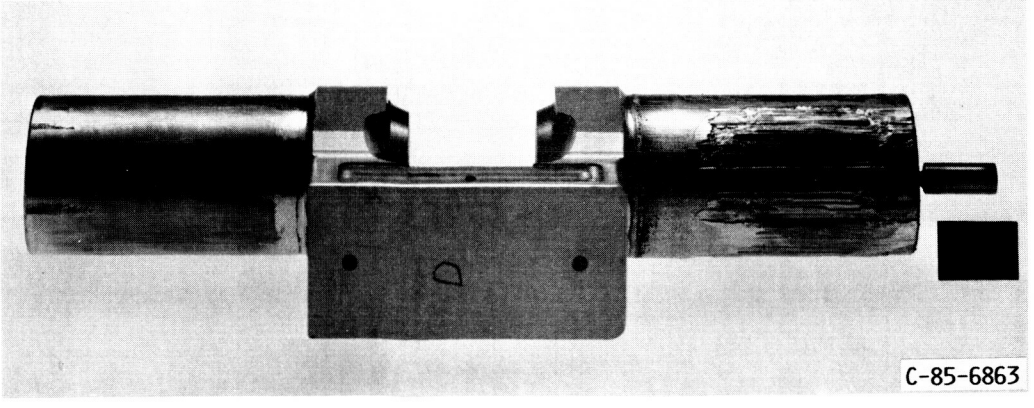

FIGURE 16. - TWO VIEWS OF FAILED CROSSHEAD FROM SECOND DRIVE-SYSTEM FAILURE.

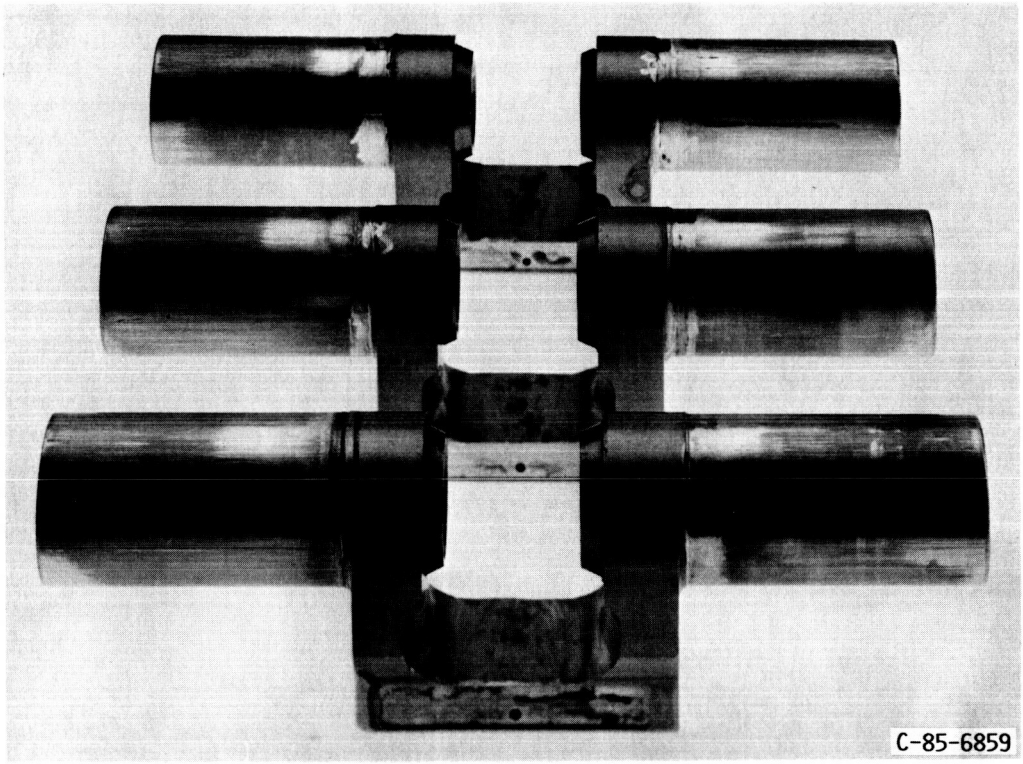

FIGURE 17. - THREE CROSSHEADS NOT PRIMARILY INVOLVED IN SECOND DRIVE-SYSTEM FAILURE.

NASA
National Aeronautics and Space Administration

Report Documentation Page

1. Report No.	2. Government Accession No.	3. Recipient's Catalog No.
DOE/NASA/50112-75 NASA TM-100899		

4. Title and Subtitle	5. Report Date
Testing of a Variable-Stroke Stirling Engine	6. Performing Organization Code

7. Author(s)	8. Performing Organization Report No.
Lanny G. Thieme and David J. Allen	E-3056
	10. Work Unit No. 778-35-13

9. Performing Organization Name and Address	11. Contract or Grant No.
National Aeronautics and Space Administration Lewis Research Center Cleveland, Ohio 44135-3191	13. Type of Report and Period Covered Technical Memorandum
12. Sponsoring Agency Name and Address U.S. Department of Energy Office of Vehicle and Engine R&D Washington, D.C. 20545	14. Sponsoring Agency Code

15. Supplementary Notes

Final Report. Prepared under Interagency Agreement DE-AI01-85CE50112. Lanny G. Thieme, NASA Lewis Research Center and David J. Allen, Sverdrup Technology, Inc., NASA Lewis Research Center Group, Cleveland, Ohio 44135. Prepared for the 21st Intersociety Energy Conversion Engineering Conference (IECEC), cosponsored by the ACS, SAE, ANS, ASME, IEEE, AIAA, and AIChE, San Diego, California, August 25-29, 1986.

16. Abstract

Testing of a variable-stroke Stirling engine at NASA Lewis has been completed. In support of the U.S. Department of Energy's Stirling Engine Highway Vehicle Systems Program, the engine was tested for about 70 hr total with both helium and hydrogen working fluids over a range of pressures and strokes. A direct comparison was made of part-load efficiencies obtained with variable-stroke and variable-pressure operation. Two failures with the variable-angle swash-plate drive system limited testing to low power levels. These failures are not thought to be caused by problems inherent in the variable-stroke concept but they do emphasize the need for careful design in the area of the crossheads where the failures occurred. This paper describes these failures and the efforts to resolve the associated problems, and presents test results that were obtained.

17. Key Words (Suggested by Author(s))	18. Distribution Statement
Stirling engine; Variable stroke; Stirling cycle; Swash plate; Heat engine	Unclassified - Unlimited Subject Category 85 DOE Category UC-96

19. Security Classif. (of this report)	20. Security Classif. (of this page)	21. No of pages	22. Price*
Unclassified	Unclassified	28	A03

*For sale by the National Technical Information Service, Springfield, Virginia 22161